Journal of Statistical Physics, Vol. 66, Nos. 3/4, 1992

Overcoming Artificial Spatial Correlations in Simulations of Superstructure Domain Growth with Parallel Monte Carlo Algorithms

W. Schleier,[1] G. Besold,[1] and K. Heinz[1]

Received July 1, 1991

We study the applicability of parallelized/vectorized Monte Carlo (MC) algorithms to the simulation of domain growth in two-dimensional lattice gas models undergoing an ordering process after a rapid quench below an order–disorder transition temperature. As examples we consider models with 2×1 and $c(2 \times 2)$ equilibrium superstructures on the square and rectangular lattices, respectively. We also study the case of phase separation ("1×1" islands) on the square lattice. A generalized parallel checkerboard algorithm for Kawasaki dynamics is shown to give rise to artificial spatial correlations in all three models. However, only if *super*structure domains evolve do these correlations modify the kinetics by influencing the nucleation process and result in a reduced growth exponent compared to the value from the conventional heat bath algorithm with random single-site updates. In order to overcome these artificial modifications, two MC algorithms with a reduced degree of parallelism ("hybrid" and "mask" algorithms, respectively) are presented and applied. As the results indicate, these algorithms are suitable for the simulation of superstructure domain growth on parallel/vector computers.

KEY WORDS: Monte Carlo algorithms; 2D lattice gas models; 2D Ising model; domain growth; phase separation; Kawasaki dynamics; parallel computer; vector computer.

1. INTRODUCTION

The kinetics of nonequilibrium systems undergoing ordering processes, such as domain growth and phase separation, is of current interest in surface physics. For systems rapidly quenched below an order–disorder transition temperature it is now widely accepted that the average domain

[1] Lehrstuhl für Festkörperphysik, Universität Erlangen-Nürnberg, D-8520 Erlangen, Germany.

0022-4715/92/0200-1101$06.50/0

size $R(t)$ represents a typical length scale describing the main physical features of the growth. By analogy to static critical phenomena, it has been proposed that different growth laws for $R(t)$ and the scaling function of the structure factor may partition various physical systems into *dynamical* universality classes, but we are still far from a complete understanding of the basis for the determination of these classes. The kinetics of domain growth and phase separation was studied both experimentally[1–13] and analytically,[14–23] but most of the contributions came from Monte Carlo (MC) simulations of spin and lattice gas models.[24–41] For reviews see, e.g., refs. 1 and 42 and references therein.

For the calculation of equilibrium properties very fast MC methods have been developed and successfully applied; among them are techniques for constructing fast algorithms suitable for vector computers or multiprocessor systems[43–52] (e.g., vectorizable algorithms with multispin coding) or new methods applying to special cases such as critical slowing down (e.g., the Swendsen–Wang algorithm[53] and the extension made by Wolff[54]). The efficiency of algorithms in both groups originates in the more or less distinguished use of parallel or—in the case of vector processors—"quasiparallel" updates of whole groups of lattice sites (sublattices) instead of single sites. If detailed balance holds, thermal equilibrium will be reached in the course of the simulated Markov chain regardless of which transition probability is used. However, if one is interested in the *kinetics* of phase transitions, the underlying physical model of time evolution must be considered and therefore artificial kinetics such as the cluster flips of the Swendsen–Wang algorithm cannot be used to simulate a system in contact with a heat bath. The picture of phonons which transfer energy to single atoms by inelastic random scattering is described best by the dynamical evolution simulated by the Metropolis algorithm in which the lattice sites are visited at random. Hence, even parallelized or vectorized versions of this standard algorithm may influence the outcoming kinetics because of artificial spatial corrections which are introduced by parallel updates. But apart from a few studies of the ferromagnetic Ising model[31,37] and the anisotropic next-nearest-neighbors Ising (ANNNI) model,[39,40] a systematic investigation considering the applicability of parallel or vectorized algorithms, especially with respect to the kinetics of *super*structure domain growth, to our knowledge is missing.

We therefore studied the influence of parallelization in simulations of domain growth kinetics in three different two-dimensional lattice gas models described in the following section. We will also discuss the relationship between computational techniques and the effectively simulated dynamics of the system under consideration. In Section 3 some fundamental effects of spatial correlations on domain growth in a lattice gas model

with 2×1 equilibrium superstructure are reported. In Section 4 we generalize these findings to other lattice gas models. In the last section we propose improvements for parallelized MC algorithms which are shown to be able to overcome artificial spatial correlations.

2. MODELS

2.1. Lattice Gas Models

In this study we used three different lattice gas models on a rectangular/square lattice of linear size L. All models can be described by a Hamitonian H with nearest neighbor interactions,

$$H = -\sum_{i,j=1}^{L} \varepsilon_1 c_{ij} c_{i+1,j} - \sum_{i,j=1}^{L} \varepsilon_2 c_{ij} c_{i,j+1} \tag{1}$$

where c_{ij} are occupation numbers and periodic boundary conditions are applied. Depending on the lateral pair interaction parameters $\varepsilon_{1,2}$, we obtain the lattice gas models I–III which are characterized in Table I.

We used a linear lattice size $L = 64$ and applied typically 300–500 independent MC runs except for some tests with $L = 256$ in order to check for finite-size effects. This proved to be sufficient for a correct valuation of the different algorithms under consideration. First we concentrate on the case of a 2×1 superstructure on a rectangular lattice with attractive as well as repulsive interactions, which are anisotropic in strength and give rise to anisotropic domain growth. Second, we compare the results of these simulations with the kinetics of two well-known systems, choosing lattice gas models which are isomorphic to the kinetic Ising model with

Table I. Lattice Gas Models with Pair Interaction Parameter ϵ_1 (y Direction) and ϵ_2 (x Direction)[a]

Model	Superstructure	$\varepsilon_1, \varepsilon_2$	Lattice	n
I	2×1	$\varepsilon_1 > 0$; (attractive) $\quad \varepsilon_2 = -1/3\varepsilon_1 < 0$ (repulsive)	Rectangular	1/2
II	$c(2 \times 2)$	$\varepsilon_1 = \varepsilon_2 < 0$ (repulsive)	Square	1/2
III	No superstructure, 1×1 islands	$\varepsilon_1 = \varepsilon_2 > 0$ (attractive)	Square	1/3

[a] n is the value of the growth exponent expected from phenomenological theories.

ferromagnetic and antiferromagnetic interactions, respectively. As the existence or absence of superstructures in the thermal equilibrium seems to be important, we consider both cases. The ordering process is studied using Kawasaki ("hopping") dynamics with nearest neighbor exchange at constant coverage $\theta = \frac{1}{2}$. We consider thermal quenches from "infinitely high" temperature (corresponding to random start configurations) to a temperature $T/T_c = 0.6$ well below the order–disorder transition.

From theoretical predictions and MC calculations the average linear size of ordered domains R is expected to obey an algebraic growth law $R(t) = a(T)t^n$ (*after* a "nucleation" phase has passed and *before* the finite lattice size becomes important) with a *kinetic* or *growth exponent* n determined by the *dynamical* universality class of the system under consideration. If the microscopic dynamics is based on translational diffusion (particle–vacancy exchanges), the order parameter is intrinsically conserved for model III and nonconserved for models I and II. For conserved order parameter and long-range diffusion (model III) systems have been found to follow the Lifshitz–Slyozov[14] behavior with $n = \frac{1}{3}$, whereas the curvature-driven growth mode described by Lifshitz[15] and Allen and Cahn[16] with $n = \frac{1}{2}$ applies in the case of nonconserved order parameter (models I and II). The average linear domain size R was measured in three different ways:

As a first measure (which can be used only for models I and II), we calculated the quantity $\langle |\Psi(t)| \rangle L =: R_\Psi(t)$ from the modulus of the order parameter Ψ, averaged over independent Monte Carlo runs at time t (L denotes the linear lattice size as introduced above). The order parameter Ψ of a *single* lattice gas configuration is defined in the sense of a "staggered occupation density," that is, as the difference of the densities of occupied sites of the two sublattices defined by the superstructure under consideration (see Fig. 3 for model I; in the case of model II the two sublattices are given by the "black" and "white" sites of a checkerboardlike partition). As a second measure for R we used the quantity $R_E(t) := 2\langle \Delta E(t) \rangle^{-1} = 2[\langle E(t) \rangle - E_{\text{eq}}(T)]^{-1}$ derived from the reciprocal average excess energy $\Delta E(t)$ per lattice site at time t [where $E_{\text{eq}}(T)$ is the average equilibrium internal energy per lattice site for the quench temperature T]. The third measure for R is the first crossing of the θ^2 level (=asymptotic value for $r \to \infty$) of the pair correlation function $G(\mathbf{r}) = \langle c_0 c_{\mathbf{r}} \rangle$ at time t, which is denoted by $R_G(t)$. In the subsequent discussions the subscripts Ψ, E, and G will be occasionally omitted if we do not want to make reference to the method used to evaluate R.

2.2. Computational Techniques

The algorithms discussed in this work make use of parallel computing, which, as we aim to show, can cause considerable errors in the simulation of ordering kinetics. We will propose solutions for this problem, however, without introducing specialized (and very fast) algorithms taking care of special hardware features or using operations on the lowest bit-level and so on. Such codes could easily be constructed from the ideas presented below. As a consequence, the speed of the algorithms discussed in Section 5 is only about 2×10^6 attempted jumps per sec including the times for the calculation of energy, order parameter, correlation function, and structure factor.

The conventional way of parallelization/vectorization is to consider either several jumps in parallel (=at the same time) on a SIMD-multiprocessor system (e.g., AMT-DAP), or only "quasiparallel" (in an inner loop) on a vector computer (e.g., CRAY Y-MP). For simplicity, we speak of "parallel" algorithms in both cases. However, parallelization forces restrictions upon the minimal distance of sites updated at the same time step. If the distance between lattice sites exceeds a lower bound—determined by the range of lateral interactions as well as the range of allowed jumps [to nearest-neighbor (NN) sites, next-nearest-neighbor (NNN) sites,...]—the sites are called "*independent.*" This leads to a generalization of the checkerboard principle[45,46] which implies that independent sites are regularly distributed over the lattice, forming S interpenetrating "update sublattices" or "U-sublattices" (with $S \geqslant 8$ for NN interaction and NN jumps on a square lattice). These sublattices are randomly selected during a Monte Carlo step (MCS) and from all occupied sites within the selected sublattice a jump is attempted in a direction which is chosen randomly for every inspected site. It appears already from a naive point of view that during this procedure artificial spatial correlations can be introduced with a periodicity given by the regular U-sublattices.

This is expressed more precisely in terms of master equations, which are very different for serial (=random) and for parallel update procedures.[31,39] Although there are some indications that Monte Carlo time scales for different update algorithms are linearly related if spatially local decision criteria are used, no rigorous proof of this statement exists.[39,50,55] Another criterion requires that there must be no significant "evolution" of the system during a Monte Carlo step if the standard master equation should be (approximately) simulated by a parallel algorithm. A necessary condition is,[31] e.g., for $R(t)$,

$$|Q| := \left| \frac{R(t+1) - R(t)}{R(t)} \right| \ll 1 \tag{2}$$

where t is measured in Monte Carlo steps. We will see in Section 3 that this condition is violated immediately after the quench when standard parallel schemes are used. Hence, the only way to test parallel algorithms is to compare their results with the conventional single-site random-updating algorithm, which will be done below.

The conventional serial algorithm is approached by increasing the number of U-sublattices S, but then the degree of parallelism is reduced, too. The task is therefore to find a compromise between these effects.

3. FUNDAMENTAL EFFECTS OF SPATIAL CORRELATIONS

In this section we restrict consideration to model I, i.e., a rectangular lattice with a 2×1 superstructure. We consider several algorithms with an increasing number S of U-sublattices. A serial random-updating algorithm with $L = 64$ and 1500 runs (resulting in a kinetic growth exponent of $n = 0.492 \pm 0.013$ from the evaluation of R_ψ) is used as a reference for comparison. As outlined in Section 2.1, we use different measures for the domain size. For each time t their average value as well as the corresponding fluctuation amplitude [e.g., $\langle |\Psi(t)| \rangle$ and $\langle \Delta |\Psi(t)| \rangle$] are calculated. Both quantities are used to determine the best-fit parameters of a power law, as well as the errors of the fit parameters. For R_ψ we actually had to consider an offset $R_\psi(t=0)$—fitting effectively $R_\psi(t) = at^n + R_\psi(t=0)$—because for finite systems the average modulus of the order parameter for $T = \infty$ (the ensemble from which the starting configuration is drawn) is not exactly zero.

In a first step we decomposed the lattice into eight sublattices (see Fig. 3), which is the minimum number of NN interactions and NN jumps. Comparing the results for the time dependence of R_ψ with the results obtained by a serial algorithm, we see that a larger value for R_ψ results for all times of the simulation (Fig. 1a). The log-log plot (Fig. 1b) shows that (i) the relative difference between the serial and the $(S = 8)$-algorithm has a maximum already after one MCS and decreases with increasing time, and (ii) in the period of 100–5000 MCS a power law seems to be still valid but with a considerably reduced growth exponent $n = 0.30 \pm 0.02$. Checking for Eq. (2) results in $Q = 4.19$ (!) for the first step, whereas for larger times, Q becomes identical to values of the serial algorithm within the error bars. This indicates that, at least at the very beginning, the parallelized algorithm is effectively simulating another master equation with another dynamical time evolution. The different values of the growth exponent n show that the relation between the two time scales is not a linear one. One might argue that the nucleation period is excluded anyway, since a universal behavior with a power law is not expected until the domain size $R(t)$ is the

dominating length scale in the system. But obviously the initial disturbance is big enough and flattens out with such a long relaxation time that even the long-time behavior is strongly affected. Furthermore, if no test for comparison is made, we encounter the misleading circumstance that a time regime with a power-law behavior could be identified; however, the resulting exponent is completely wrong.

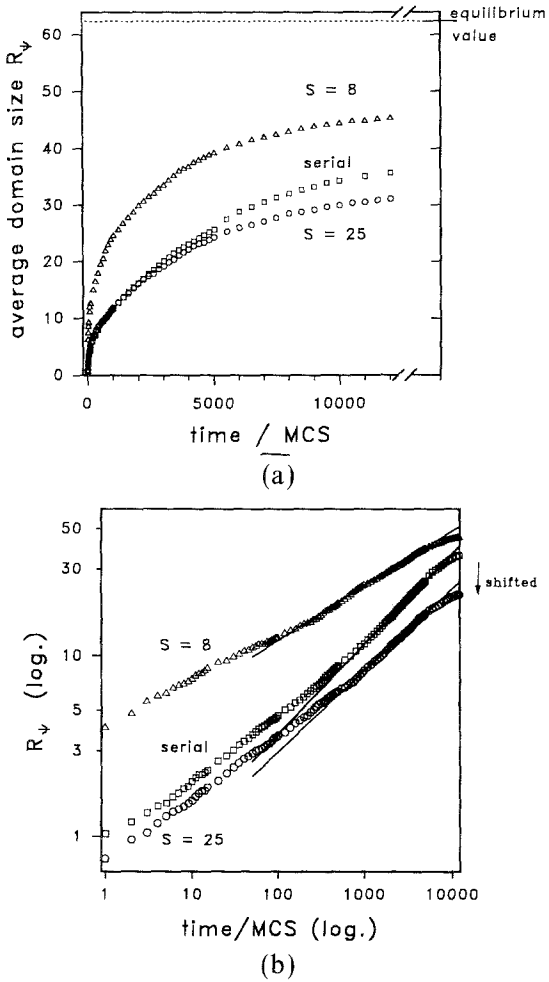

Fig. 1. (a) Linear and (b) log-log plot of the time dependence of the average domain size R_Ψ for model I (2×1 superstructure, $L = 64$) for different updating procedures: (□) random/serial, (△) checkerboard with $S = 8$, and (○) checkerboard with $S = 25$. The straight lines in (b) are fits to a power law with exponents $n = 0.49$, 0.30, and 0.45 for serial, $S = 8$, and $S = 25$ algorithms, respectively. The curve for $S = 25$ is shifted for clarity as indicated by the arrow. $R_\Psi = \langle |\Psi| \rangle L$, i.e., $R_\Psi = 64$ corresponds to $\Psi = 1$.

When the number of U-sublattices is increased to $S=25$, a behavior of $R_\psi(t)$ more similar to the serial algorithm is observed (cf. Fig. 1). The kinetic exponent $n=0.45\pm0.02$ is closer to its predicted value $\frac{1}{2}$, just as the quotient Q approaches values resulting from the serial algorithm. This makes one expect that the results might generally be improved when the number of U-sublattices S is increased (degree of parallelism decreased). However, as shown in Fig. 2a, this is not the case, but an oscillating trend is observed instead or, in other words, two different curves can be identified. In Fig. 2a these curves are denoted by "misfit" and "fit," respectively. (The meaning of this labeling will become clear in a moment.) In order to understand the reason for the existence of *two* curves, Fig. 3 shows the *two* sublattices (A and B) defined by the 2×1 superstructure: there are two

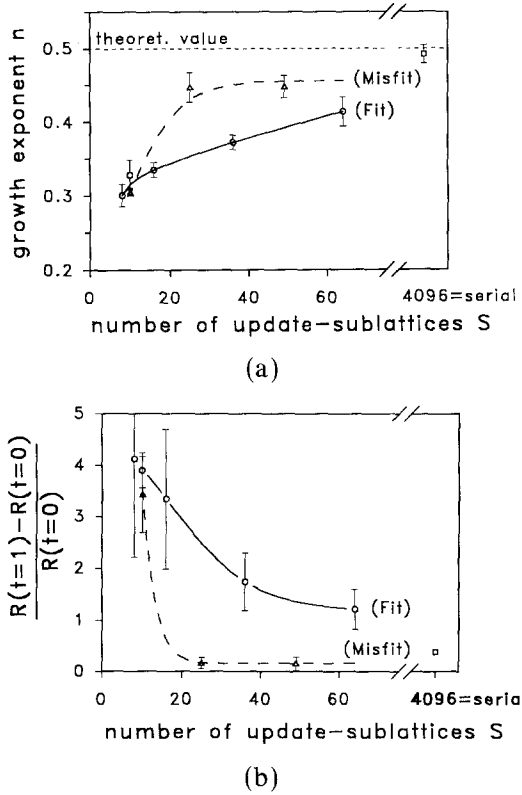

Fig. 2. (a) Growth exponents and (b) quotient Q defined in Eq. (2) for varying numbers of U-sublattices S in the generalized checkerboard algorithm for model I (2×1 superstructure, $L=64$). Curves only serve as guidelines. The error bar of the last data point in (b) is smaller than the symbol size.

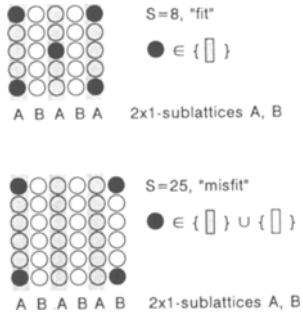

Fig. 3. Different positions of U-sublattices relative to 2×1 superstructure sublattices for $S=8$ and $S=25$ (see also text): filled circle (●) mark sites belonging to one of S U-sublattices, dark and light rows indicate the 2×1 sublattices.

antiphase domains possible and in each domain type one "2×1 *sublattice*" is occupied (e.g., A) and the other is empty (e.g., B). One can imagine that it is important whether all sites of a "U-sublattice" reside on the same "2×1 sublattice" (defining the curve denoted by "fit") or whether the sites reside alternating on both "2×1 sublattices" (defining the curve denoted by "misfit"). In this context it is very informative to look at Fig. 2b, where the quotient $Q(t=0)$ is plotted versus the number of U-sublattices S. A correlated behavior becomes visible: The "worse" the algorithm (measured by the deviation of the growth exponent n from its serial value), the less Eq. (2) holds. This is true not only for values of Q which are too high, but also if Q is slightly to low (e.g., for $S=25$, 49). The latter case may be an indication of an inhibitory effect on the order-forming process. Both effects, enforcing or inhibiting growth, will result in a modified kinetics.

As we will see, strong artificial spatial correlations can be detected in all cases (i.e., number of U-sublattices S); however, they strongly influence the kinetics only if the U-sublattices and the superstructure sublattices fit together (in the meaning of Fig. 3). This effect can directly be observed by looking at the short-time behavior of the pair correlation function $G(\mathbf{r})$ (see Fig. 4 for $S=16$; the direction $\mathbf{r}$ shown here is normal to the 2×1 rows). The starting point is a random distribution of occupied sites with the probability of finding a particle given by the coverage $\theta = \frac{1}{2}$ [thus, $G(\mathbf{r}) \equiv \theta^2 = \frac{1}{4}$]. The shape after 500 MCS, which is taken for comparison from the serial algorithm, shows already the developing superstructure of occupied and empty rows (Fig. 4b). If we take the "staggered" pair correlation function [by reflecting every second point at the line $G(\mathbf{r}) = \theta^2 = 0.25$], all data fall on the single solid curve showing a shape well known from the

ferromagnetic Ising model. On the other hand, a rather strange picture arises already after the *first* MCS for the ($S=16$)-algorithm. The cases $S=16$ means that the U-sublattice has a lattice constant of four times the lattice spacing—exactly the periodicity of 4 found in $G(\mathbf{r})$. A full period is marked by a dotted line in Fig. 4c and has itself a modulation with "periodicity" 2, indicating short-range order of alternating occupied and empty sites. After 100 MCS a *simultaneous* formation of the 2×1 order over the *whole* lattice can be observed (Fig. 4d). This is equivalent to high initial values of $R(t)$, which then cause the reduced exponent n (cf. Fig. 1b). A coupling of this type is not possible if the superstructure and the U-sublattices do not fit together.

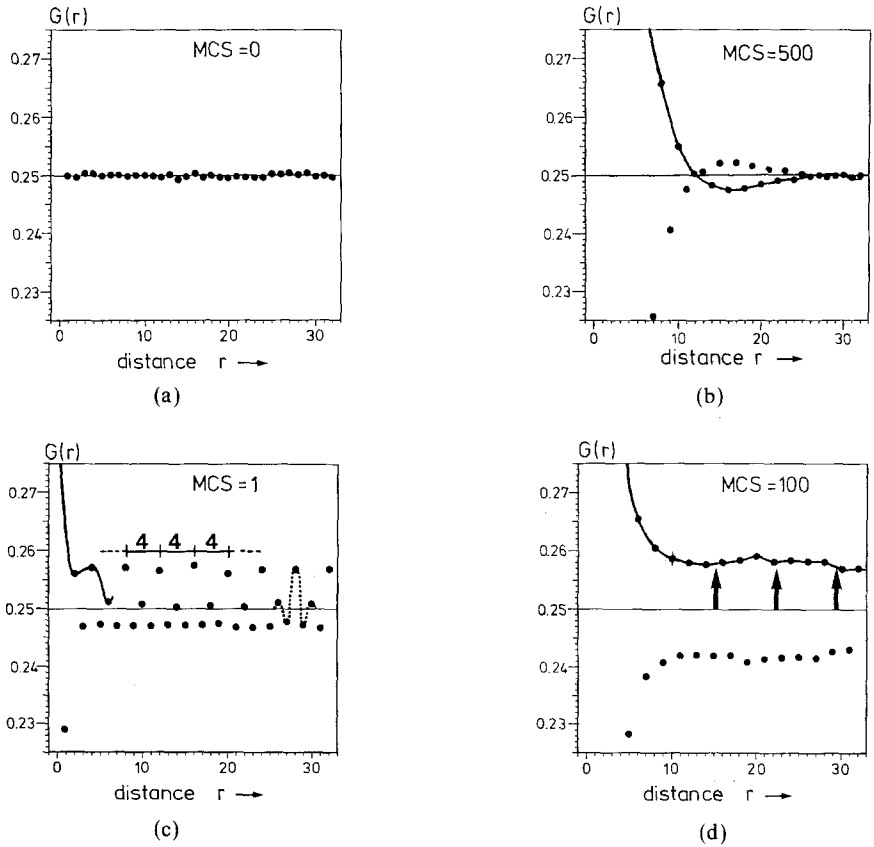

Fig. 4. Short-time behavior of the pair correlation function $G(\mathbf{r})$ in the direction normal to the developing rows of the 2×1 structure: (a) starting point ($t=0$ MCS), (b) random/serial algorithm after $t=500$ MCS, (c) $S=16$ checkerboard at $t=1$ MCS, and (d) same as (c), at $t=100$ MCS.

The conclusion is therefore always to choose U-sublattices which do not fit to the sublattices defined by the superstructure. If such a subdivision is not possible (e.g., when the quench is performed into a coexistence region of two phases with different periodicities) or if an algorithm is desired which is generally applicable, independent of the structure under consideration, the slow convergence toward the correct value $n = \frac{1}{2}$ (demonstrated in Fig. 2a) makes a more sophisticated algorithm necessary. A last remark of this section refers to possible "fingerprint" measures of the difference between a parallel algorithm and the serial one. The simplest way is to calculate the difference in $R(t)$ at each time t and then to sum up (over all times) the modulus or the square of that deviation. We found additionally that the amount of the reduction of the kinetic growth exponent n is a very sensitive measure, too, which gives almost the same information and which will therefore be used in the following sections.

4. TEST OF OTHER MODELS

In this section we show the above results to be general, i.e., they not only hold for model I, but also for other lattice gas or spin models. We expect qualitatively the same effects for every model with *super*structure domains, whereas in the absence of a superstructure the kinetics should be independent of the algorithm under consideration. This idea suggests that one investigates in a next step a model which shows the formation of a superstructure, too.

4.1. Presence of Superstructure

We choose a lattice gas model isomorphic to the well-known antiferromagnetic Ising spin model. According to the nonconservation of the order parameter in this case, the theoretically predicted value for the kinetic exponent is again $n = \frac{1}{2}$. As a reference we again used a serial random-updating version and from the evaluation of R_ψ we found $n = 0.52$ in only 200 runs. Afterward we switched to a parallel algorithm with $S = 8$ and looked at the time dependence of R_ψ. As for model I, the order parameter values are much higher than in the serial case, but as demonstrated in Fig. 5, no power law is valid for the full time scale. With increasing time the locally fitted values for n drop continuously from $n = 0.26$ at the beginning. This low kinetic exponent nicely confirms our interpretation of the previous section. The fact that for model II [$c(2 \times 2)$ superstructure] the influence of the artificial correlations is stronger and that the—locally defined—exponent is below the value for model I (2×1 superstructure) can be explained as follows: Going along the directions

marked by the lateral interactions, one finds a periodicity 2 in *both* directions for model II, whereas for model I, only along the direction of repulsive interaction, i.e., across the 2×1 rows, does a periodicity 2 appear. If, on the other hand, a misfit between the superstructure and the U-sublattices will occur (e.g., $S = 25$), this misfit extends in *both* directions for model II and gives a time evolution which is more similar to the serial

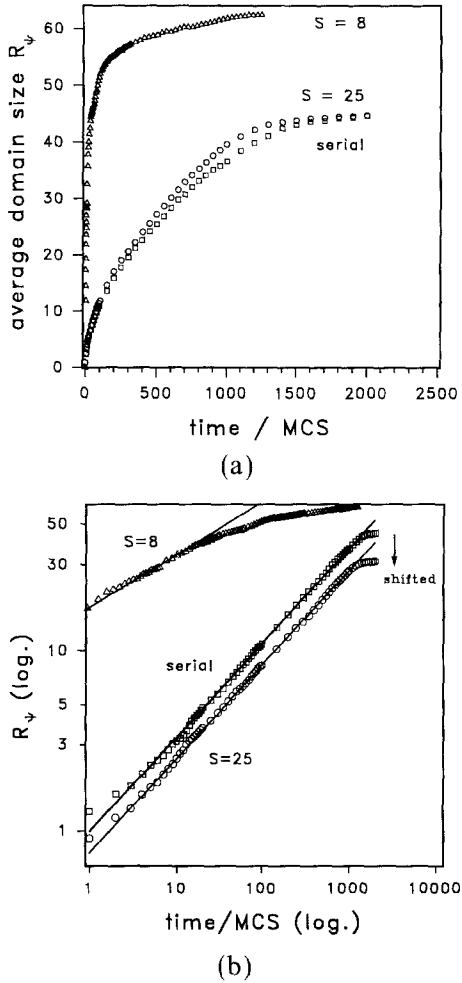

Fig. 5. (a) linear and (b) log-log plot of the time dependence of the average domain size R_ψ for model II [$c(2 \times 2)$ superstrcture] for different update procedures (serial and $S = 25$: lattice size $L = 64$; $S = 8$: rescaled results for $L = 256$): (□) random/serial, (△) checkerboard with $S = 8$, and (○) generalized checkerboard with $S = 25$. The straight lines in (b) represent the fitted algebraic growth law with exponents $n = 0.52$, 0.26, and 0.52 for serial, $S = 8$, and $S = 25$ algorithms, respectively. The curve for $S = 25$ is shifted for clarity as indicated by the arrow.

algorithm as for model I with $S=25$. This supports strongly the idea that the relationship between a superstructure periodicity and a U-sublattice periodicity is decisive for the quality of the algorithm.

When we use the reciprocal excess energy ΔE^{-1} to measure R, we get similar results. One difference is that the reduction of the exponent is less drastic ($n=0.42$) than for R_Ψ; the other is that the considerable changes in the "nucleation" period seen by R_Ψ are not detectable by evaluating R_E and that only the long-time behavior is modified. This discrepancy in the exponents according to different measures of R may help one to recognize a "wrongly" working parallel algorithm. But this discrepancy raises the question of whether the algebraic growth regime is reached or not, because from this time on, all length scales and derived exponents should be equivalent. Since the difference in the exponents holds even in simulations with a linear lattice size $L=256$, we believe that the effect is caused mainly by spatial correlations in the parallel algorithms.

In the literature[39,40] the same generalized checkerboard method was applied to a very similar model, the Ising model with antiferromagnetic interactions, but with Glauber (spin-flip) instead of Kawasaki (spin-exchange) kinetics. The authors of refs. 39 and 40 found no deviations from the serial results when they used an algorithm with $S=16$ and measured the domain size via the excess energy. We evaluated the kinetic exponent for $S=16$, too, but using Kawasaki kinetics, and found n to lie far below the theoretical value $n=\frac{1}{2}$ ($n=0.38\pm0.02$ for R_E and $n\leqslant 0.39$ for R_Ψ, only locally defined exponents). To search for reasons why the serial and the ($S=16$)-algorithm give different results only for Kawasaki kinetics and not for Glauber kinetics, we tested several pseudo-random-number generators (for $S=8$ and model I): a linear congruential generator for a 32-bit processor[56] ($x_{i+1}=ax_i \bmod m$ with $m=2^{31}$ and $a=331{,}804{,}469$), the built-in generators "RANF" (for a CYBER 995E and a CRAY Y-MP), and "g05_mc_r4"[57] (for the processor array AMT-DAP 500) and a feedback shift register modulo generator based on the ideas of Tausworth[58] and with modifications of Kirkpatrick and Stoll[59] ($x_i=x_{i-q}.\text{xor}.x_{i-p}$ with $p=532$, $q=37$). However, all tests confirmed our previous results. So, either the effect of a modified exponent is negligibly small or nonexistent for Glauber kinetics or it remained undetected by Shah and Mouritsen[39] due to some insensitivity of the excess energy with respect to spatial correlations.

4.2. Absence of Superstructure

In the following we investigate a model without a superstructure, for which we expect no or only vanishingly small effects due to artificial spatial

correlations. Model III has the desired properties because only 1×1 islands grow. All calculations for this model were performed for a linear lattice size $L = 256$. Since the order parameter is conserved, the system should follow a Lifshitz–Slyozov growth mode with $n = \frac{1}{3}$. However, as known from previous studies,[22,23] additional basic assumptions must be incorporated into the framework of the Lifshitz–Slyozov theory in order to allow a correct interpretation of results from simulations. These theoretical "corrections" lead to modifications of the algebraic growth law for intermediate times and have to be considered in the evaluation of the true exponent n. Two possible suggestions involve corrections by additional diffusion along the domain boundaries[22] or by a reduced driving force for the domain growth due to the finite roughness of the boundaries.[23] Regarding the transport along the interfaces, a time-dependent, "effective" exponent n_{eff} appears,[22] which asymptotically converges to $\frac{1}{3}$:

$$n_{\text{eff}} = \frac{d \ln R}{d \ln t} = \frac{1}{3} - \frac{\text{const}}{R(t)} + O(R^{-2}) \tag{3}$$

If a finite roughness of the domain boundaries is included in the theory, a power law for R with an offset R_0 is valid[23] (R_0 is of the order of the finite roughness of the boundaries):

$$R(t) = a \cdot t^n + R_0 \qquad \text{with} \quad n = 1/3 \tag{4}$$

Computing the effective exponent from Eq. (4) immediately gives Eq. (3) when $R(t) \gg R_0$. Despite the different physical interpretation, the resulting effective exponents should be equal and so this agreement provides a phenomenological basis for an analysis: The true asymptotic exponent results from a fit to Eq. (4) or by a linear extrapolation of the function $n_{\text{eff}}(1/R)$ for $1/R \to 0$. To check this behavior, we applied both procedures. For the serial algorithm a fit of $R_E(t)$ to Eq. (4) (fitting n and R_0) gives $n = 0.33$ and $R_0 = 5.9$ (Fig. 6a). From the extrapolation of $R_E \to \infty$ an exponent $n = 0.33$ results (Fig. 6b). Only points for which $R_E(t) > 2R_0 \approx 12$ were used in both cases because Eqs. (3) and (4) become equivalent only if the condition $R(t) \gg R_0$ is valid and because the whole time dependence of R_E cannot be described by Eq. (4) (see the deviations in the initial phase in Fig. 6a, where the asymptotic growth is not yet reached). Because of the uncertainty in fixing the correct starting point for the fit, a relatively large error of $\Delta n = 0.03$ results. Equations (3) and (4) predict the fit to become the better the more initial values are omitted, but then the larger fluctuations of the late-time data affect the accuracy of the fit.

A few more words must be said about the determination of the effec-

tive exponents. We evaluate n_{eff} by numerical differentiation of the data on the log-log scale. Since already small fluctuations in the data cause large fluctuations in n_{eff} (cf. Fig. 7a), the original data were smoothed on the log-log scale before we determined the effective exponents (Fig. 7b). The smoothing on the double logarithmic scale was done by creating a new data point simply by calculating the "center of mass" of five successive points of raw data ($\log(t_i)$, $\log [R(t_i)]$). This smoothing procedure was chosen because a power law is invariant under this transformation. Compared to the procedure proposed by Amar *et al.*[37] (n_{eff} results from a fit in the interval $[t_i, 2t_i]$), the advantage of this procedure is to get values n_{eff} which are better localized in time. The smoothing procedure only reduces noise, but leaves extrapolated exponents unmodified within an accuracy of 1%.

For the $(S=8)$-algorithm we finally found exponents according to Eqs. (3) and (4) which are only slightly different from those of the serial algorithm and from the theoretical value $n=\frac{1}{3}$. The good agreement between serial and parallel algorithms still holds if the zeros of the spin autocorrelation function are evaluated. Nevertheless, we can still detect artificial correlations—very similar to those of model I—in the very beginning of the nucleation process (cf. Fig. 8). However, because of the missing superstructure, no coupling effect, as demonstrated in Fig. 4d, is possible

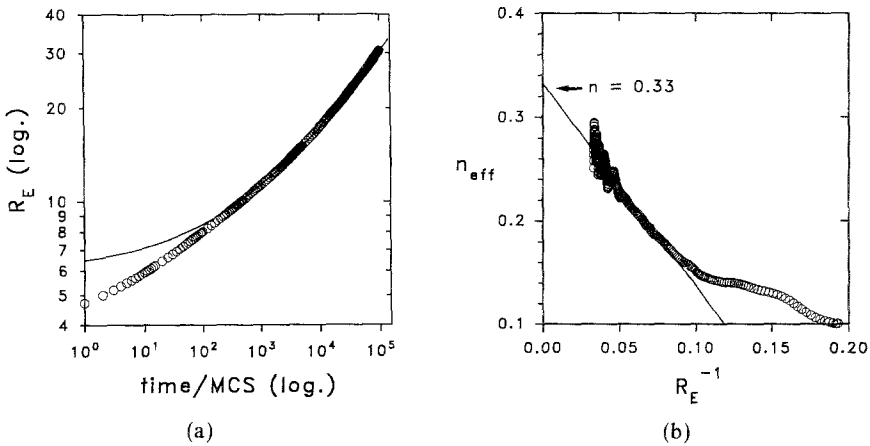

Fig. 6. (a) Log-log plot of $R_E(t)$ for model III (1×1 structure) simulated with a serial algorithm (lattice size $L=256$). The solid curve is a fit to $R_E(t)=R_0+at^n$ with $n=0.33$, $R_0=5.9$. (b) Effective exponent n_{eff} [see Eq. (3)] as a function of $1/R_E$ [same data as (a)]. The straight line is an extrapolation to $R_E\to\infty$ with result $n=0.33$ (only data for $R_E>12$ are included in the fit).

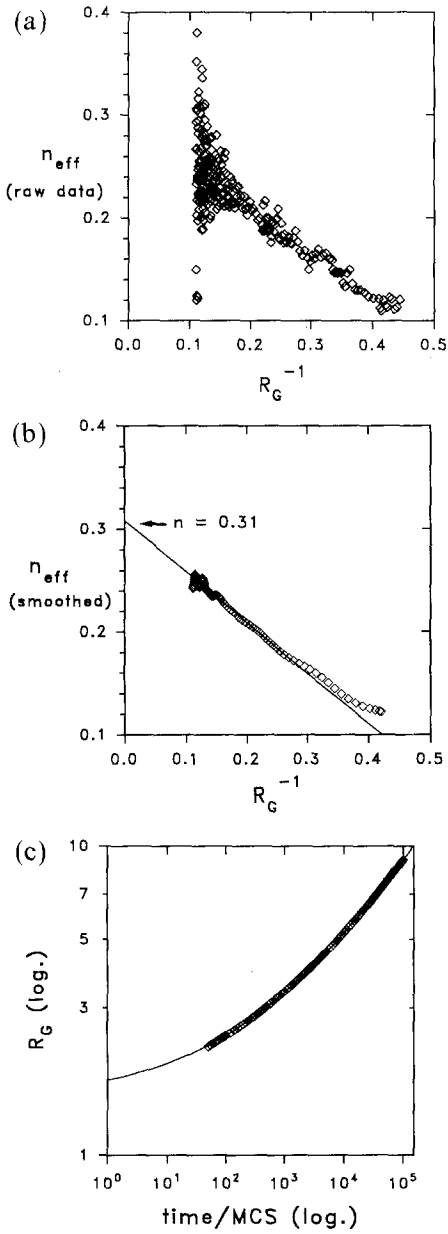

Fig. 7. (a) Raw data for the effective growth exponent n_{eff} derived after numerical differentiation [see Eq. (3)] as a function of $1/R_G$ for model III and $L=256$, simulated with a serial algorithm. (b) Effective exponent n_{eff} after smoothing of the raw data of (a) as a function of $1/R_G$. The straight line is an extrapolation for $R_G \to \infty$ (only data for $R_G > 4$ are included in the fit) with the result $n=0.31$. (c) Log-log plot of $R_G(t)$. The solid curve is a fit to $R_G(t) = R_0 + at^n$ with $n=0.31$, $R_0=1.6$.

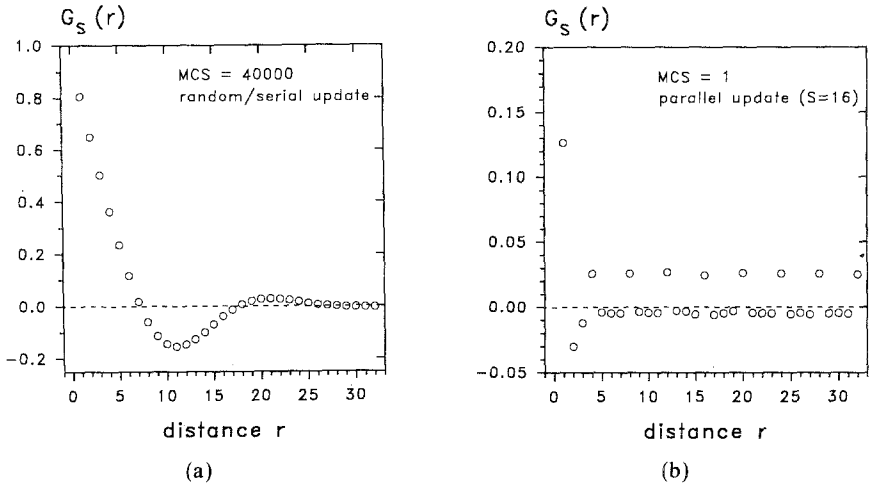

Fig. 8. Short-time behavior of the spin autocorrelation function $G_S(\mathbf{r}) = \langle s_0 s_\mathbf{r} \rangle$ in the direction of the NN interaction for model III (1×1 structure): (a) expected behavior after $t = 40000$ MCS (random/serial algorithm), (b) generalized checkerboard algorithm with $S = 16$ at $t = 1$ MCS.

and consequently the strange shape of $G(\mathbf{r})$ vanishes very soon. A part of our observations is in agreement with a previous study[37] in which an algorithm with $S = 16$ was applied (without further checks mentioned) and from which also the predicted exponent $n = \frac{1}{3}$ resulted.

5. PROPOSAL OF IMPROVED ALGORITHMS

5.1. Hybrid Algorithm

From the above results it is obvious that parallelized MC algorithms for superstructure growth kinetics should have features which reduce spatial correlations. In section 3 the reduction was done by increasing the number of U-sublattices. But because of the slow convergence of the kinetic exponent toward the theoretical value, another solution is desired. Our aim is therefore to construct an algorithm which works for a large number of lattice gas models with superstructures, regardless of their complexity. We made simulations for model I starting with an algorithm which uses the minimum number of sublattices (here: $S = 8$) and tried to improve it. The simplest way to do this is to consider only a fraction f of *randomly selected* "active" sites[39,60] of one U-sublattice at a time instead of the whole sublattice. Clearly, as the fraction f goes to zero, the artificial spatial correlations vanish and the parallelized algorithm becomes a serial one, but a

lower bound for f is given by the hardware. If the number of parallel updated sites ($=fL^2/S$) falls below the number of processors in a SIMD-processor array (e.g., AMT-DAP), the algorithm becomes inefficient. For vector processors the lower bound is less definite and approximately lies between half of and the full vector length. For example, if $L=64$, $S=8$, and the vector length is 64 (CRAY Y-MP), we get $f \geqslant 1/16 \ldots 1/8$. We decreased this fraction starting from $f=1$ (all sites within a U-sublattice) to $f=1/16$. From Fig. 9 it is obvious that a further reduction of f yields only a very slow convergence of the kinetic exponents to $n=\frac{1}{2}$.

Because of the insufficient accuracy even at $f=1/16$ (exponent $n=0.42$), we took into account that especially in the nucleation phase the system reacts very sensitive to correlations and used a serial algorithm with fully random updating in the initial phase of every run. After about 50–100 MCS the crucial time period is over and we switched to the parallel ($S=8$)-algorithm. Since the time range of "free" growth (simulated with parallel updates) was typically three magnitudes larger than the initial "nucleation" period (with serial updates), only slightly more CPU time is needed for this kind of "*hybrid algorithm*" on the CRAY Y-MP in comparison to the fully parallelized program version. On a processor array like the AMT-DAP the same hybrid algorithm is possible in principle, but the serial part of the algorithm will be less efficient than on a vector processor. Possibly it is sufficient to use only a "less parallel" version with a high number of U-sublattices S instead of a completely serial part, but we did not check this. With this modification an exponent $n=0.485 \pm 0.01$ results, which is already within the error of the serial result. An even more precise value results if roughly the same "trick" is applied again and a serial MCS is inserted every 20 parallel MCS in order to suppress residual artificial correlations. We finally found a kinetic exponent $n=0.506 \pm 0.015$ for model I with this modified parallel algorithm, which is still a factor of about four faster than a serial MC algorithm (CRAY Y-MP results).

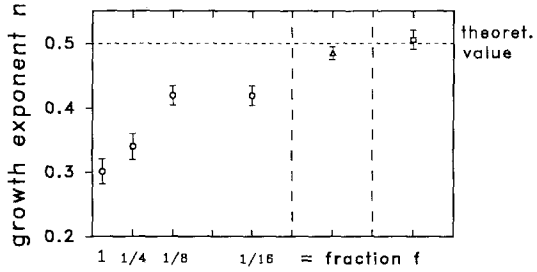

Fig. 9. Growth exponents for different "hybrid algorithms": (○) decreasing fraction f of "active" sites within a U-sublattice; (△) $f=1/16$ and nucleation period up to 100 MCS simulated by a serial algorithm; (□) additional serial MC step inserted after every 20th MCS.

5.2. Mask Algorithm

In all algorithms presented so far regular sublattices are used and the inherent spatial periodicity in the sequence of the updated sites caused crucial artificial correlations. A logical next step for an improvement is to give up the concept of regular sublattices. However, if only randomly distributed sites should be considered in parallel, their mutual independence must be checked in advance. But this cannot be done for every individual MCS, because it is a very time-consuming task, which intrinsically cannot be parallelized. The idea is to do this job only once at the beginning of each MC run and to store the information for further, repeated use. We constructed groups of *independent* sites, which are *randomly distributed* over the lattice. Such a group is called a "*mask.*" Each mask contains the same number M of independent sites (=mask size). All sites within a mask are updated in parallel; therefore the parameter M controls the degree of parallelism and is comparable to the quantity fL^2/S in the hybrid algorithms. It is clear that with an increasing mask size the arrangement of the sites within a mask will become more and more regular and for $M=L^2/S$ we will get just the same sublattices as used for the hybrid algorithms. In practice we stay far away from this upper limit for M. On the other hand, we approach the serial algorithm when the mask size goes to zero. Our masks are built in such a way that their union covers the whole lattice. For the L^2 lattice sites we get L^2/M masks, which we call a "*mask set.*" Since during the simulation less random numbers have to be calculated for these "*mask algorithms*" (only one mask is chosen instead of M single sites!), the time for the construction of the masks is compensated and so in total roughly the same CPU time is required compared to a hybrid algorithm with comparable efficiency.

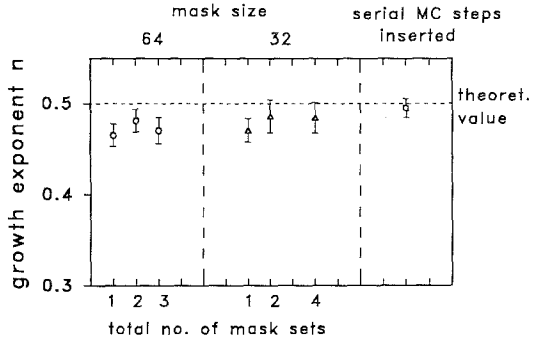

Fig. 10. Growth exponents for different "mask algorithms": (○) mask size 64 with 1, 2, or 3 mask sets; (△) mask size 32 with 1, 2, or 4 mask sets; (□) mask size 32 with 4 mask sets and additional serial MCS after every 10 MCS.

In our tests we varied the mask size ($M = 32$, 64) and the number of mask sets (1, 2, and 4) and obtained for model I kinetic exponents in the range $n = 0.46$–0.49 (see Fig. 10) for all parameters used. The exponents are only slightly improved by decreasing the mask size and increasing the number of mask sets. This means that in fact all exponents are generally very close to the serial result, but small differences are still present. A higher number of mask sets or lower values for the mask size are ruled out because of the additional memory needed for storing the masks and the reduced parallelism, respectively. In order to improve the algorithm further, we again inspected the nucleation period, but no spatial correlations were visible and therefore no corrections were needed. A further improvement is reached by inserting a serial MCS from time to time. If this is done every 10 parallel MC steps, we get an exponent $n = 0.495 \pm 0.01$ and, compared to the serial results, identical $R(t)$ curves within the errors bars.

6. SUMMARY

A generalized version of the checkerboard algorithm was used for the simulation of domain growth at fixed coverage (Kawasaki dynamics). As a consequence of parallel updates of sublattices, the evaluation of the pair correlation function for different times reveals that strong artificial spatial correlations are introduced into the system. The results of our simulations point out, however, that only in the case of *super*structure domain growth (and depending on the fit or misfit of "update" and "superstructure" sublattices) is the nucleation period distorted in a very peculiar manner. This leads to strong modifications even of the late-time behavior of the growth process and results in a considerably (up to 50%) reduced growth exponent with respect to the conventional (serial) heat-bath algorithm with random single-site updates. In contrast to the findings for the kinetics of lattice gas models with *super*structure domains, no significant change in the kinetics can be detected in the case of phase separation in a 1×1 model (without superstructure). In order to overcome the artificial modifications introduced by parallel update procedures, we developed two algorithms with gradually reduced parallelism: A "hybrid" algorithm with additionally inserted serial MC steps and a "mask" algorithm which abandons the concept of regular sublattices and uses sets of randomly distributed independent lattice sites in the parallel updating procedure instead. Our algorithms provide a reasonable compromise between an efficient use of parallel computing facilities and the applicability to the study of superstructure growth kinetics.

ACKNOWLEDGMENTS

Support by the Höchstleistungsrechenzentrum (HLRZ), Jülich, and by the Leibniz-Rechenzentrum der Bayerischen Akademie der Wissenschaften, Munich, is gratefully acknowledged. We are also indebted to the Lehrstuhl für Informatik VII, University of Erlangen-Nürenberg, for access to the AMT-DAP.

REFERENCES

1. K. Heinz, Experiments on kinetic effects at phase transitions, in *Kinetics of Interface Reactions*, M. Grunze and H. J. Kreuzer, eds. (Springer, Berlin, 1987), p. 202, and references therein.
2. K. Heinz, G. Schmidt, L. Hammer, and K. Müller, *Phys. Rev. B* **32**:6214 (1985).
3. K. Heinz, A. Barthel, L. Hammer, and K. Müller, *Surf. Sci.* **191**:174 (1987).
4. M. C. Tringides, P. K. Wu, and M. G. Lagally, *Phys. Rev. Lett.* **59**:315 (1987).
5. P. K. Wu, M. C. Tringides, and M. G. Lagally, *Phys. Rev. B* **39**:7595 (1989).
6. M. C. Tringides, *Phys. Rev. Lett.* **65**:1372 (1990).
7. J. K. Zuo, G. C. Wang, and T. M. Lu, *Phys. Rev. Lett.* **60**:1053 (1988).
8. J. K. Zuo, G. C. Wang, and T. M. Lu, *Phys. Rev. B* **39**:9432 (1989).
9. J. K. Zuo, G. C. Wang, and T. M. Lu, *Phys. Rev. B* **40**:524 (1989).
10. J. K. Zuo and G. C. Wang, *Phys. Rev. B* **40**:7078 (1990).
11. E. G. McRae and R. A. Malic, *Phys. Rev. Lett.* **65**:737 (1990).
12. B. Garni, D. E. Savage, and M. G. Lagally, *Surf. Sci.* **235**:L324 (1990).
13. H. Busch and M. Henzler, *Phys. Rev. B* **41**:4891 (1990).
14. I. M. Lifshitz and V. V. Slyozov, *J. Chem. Phys. Solids* **15**:35 (1961).
15. I. M. Lifshitz, *Sov. Phys. JETP* **5**:939 (1962).
16. S. M. Allen and J. W. Cahn, *Acta Metall.* **27**:1085 (1979).
17. G. F. Mazenko, O. T. Valls, and M. Zannetti, *Phys. Rev. B* **38**:520 (1988).
18. Z. W. Lai, G. F. Mazenko, and O. T. Valls, *Phys. Rev. B* **37**:9481 (1988).
19. G. F. Mazenko, *Phys. Rev. B* **42**:4487 (1990).
20. T. Ohta, D. Jasnow, and K. Kawasaki, *Phys. Rev. Lett.* **49**:1223 (1982).
21. A. Milchev, K. Binder, and D. W. Heermann, *Z. Phys. B* **63**:521 (1986).
22. D. A. Huse, *Phys. Rev. B* **34**:7845 (1986).
23. C. Yeung, *Phys. Rev. B* **39**:9652 (1989).
24. M. K. Phani, J. L. Lebowitz, M. H. Kalos, and O. Penrose, *Phys. Rev. Lett.* **45**:366 (1980).
25. P. S. Sahni, G. Dee, J. D. Gunton, M. Phani, J. L. Lebowitz, and M. Kalos, *Phys. Rev. B* **24**:410 (1981).
26. P. S. Sahni and J. D. Gunton, *Phys. Rev. Lett.* **47**:1754 (1981).
27. P. S. Sahni, D. J. Srolovitz, G. S. Grest, P. Anderson, and S. A. Safran, *Phys. Rev. B* **28**:2705 (1983).
28. K. Kaski, M. C. Yalabik, J. D. Gunton, and P. S. Sahni, *Phys. Rev. B* **28**:5263 (1983).
29. A. Sadiq and K. Binder, *J. Stat. Phys.* **35**:517 (1984).
30. J. Viñals and J. D. Gunton, *Surf. Sci.* **157**:473 (1985).
31. E. T. Gawlinski, M. Grant, J. D. Gunton, and K. Kaski, *Phys. Rev. B* **31**:281 (1985)
32. E. T. Gawlinski, M. Grant, J. D. Gunton, and K. Kashi, *Phys. Rev. B* **32**:1575 (1985).
33. O. G. Mouritsen, *Phys. Rev. Lett.* **56**:850 (1986).
34. T. Ala-Nissila and J. D. Gunton, *Phys. Rev. B* **33**:7583 (1986).
35. T. Ala-Nissila and J. D. Gunton, *Phys. Rev. B* **38**:11418 (1988).

36. G. S. Grest and M. P. Anderson, *Phys. Rev. B* **38**:4752 (1988).
37. J. G. Amar, F. E. Sullivan, and R. D. Mountain, *Phys. Rev. B* **37**:196 (1988).
38. H. C. Kang and W. H. Weinberg, *Phys. Rev. B* **41**:2234 (1990).
39. P. J. Shah and O. G. Mouritsen, *Phys. Rev. B* **41**:7003 (1990).
40. O. G. Mouritsen, P. J. Shah, and J. V. Andersen, *Phys. Rev. B* **42**:4506 (1990).
41. W. Schleier, G. Besold, and K. Heinz, *Vacuum* **41**:412 (1990).
42. M. G. Lagally, ed., *Kinetics of Ordering and Growth at Surfaces* (Plenum Press, New York, 1990).
43. L. Jacobs and C. Rebbi, *J. Comp. Phys.* **41**:203 (1981).
44. R. Zorn, H. J. Herrmann, and C. Rebbi, *Comp. Phys. Commun.* **23**:337 (1981).
45. W. Oed, *Appl. Informatics* 7:358 (1982).
46. S. Wansleben, J. G. Zabolitsky, and C. Kalle, *J. Stat. Phys.* **37**:271 (1984).
47. G. Bhanot, D. Duke, and R. Salvador, *J. Stat. Phys.* **44**:985 (1986).
48. F. Sullivan and R. D. Mountain, A fast MPP algorithm for Ising spin exchange simulations, in *Frontiers of Massively Parallel Scientific Computation*, J. R. Fischer, ed. (NASA Conference Publication No. 2478, 1987), p. 53.
49. M. Q. Zhang, *J. Stat. Phys.* **56**:939 (1989).
50. D. W. Heermann and A. N. Burkitt, Parallelization of computational physics algorithms, in *Computer Simulation Studies in Condensed Matter Physics II*, D. P. Landau, K. K. Mon, and H.-B. Schüttler, eds. (Springer, Berlin, 1990), p. 16.
51. G. S. Pawley and G. W. Thomas, *J. Comp. Phys.* **47**:165 (1982).
52. S. F. Reddaway, D. M. Scott, and K. A. Smith, *Comp. Phys. Commun.* **37**:351 (1985).
53. R. H. Swendsen and J.-S. Wang, *Phys. Rev. Lett.* **58**:86 (1987).
54. U. Wolff, *Phys. Rev. Lett.* **62**:361 (1989).
55. H. A. Ceccatto, *Phys. Rev. B* **33**:4734 (1986).
56. N. Schmitz and F. Lehmann, *Monte Carlo Methods I—Generating and Testing of Pseudo Random Numbers* (Anton Hain, Meisenheim/Glan, 1976), p. 47.
57. K. A. Smith, S. F. Reddaway, and D. M. Scott, *Comp. Phys. Commun.* **37**:239 (1985).
58. R. C. Tausworth, *Math. Comput.* **19**:201 (1965).
59. S. Kirkpatrick and E. P. Stoll, *J. Comp. Phys.* **40**:517 (1981).
60. W. Schleier, G. Besold, and K. Heinz, Parallel Monte Carlo algorithms for domain growth kinetics, in *Proceedings of the CP 90 Europhysics Conference on Computational Physics*, A. Tenner, ed. (World Scientific, Singapore, 1991), p. 468.